The Journal of Experimental Biology 211, 1937-1947
Published by The Company of Biologists 2008
doi:10.1242/jeb.014217

The effect of proline on the network structure of major ampullate silks as inferred from their mechanical and optical properties

Ken N. Savage and John M. Gosline*

Department of Zoology, 6270 University Boulevard, University of British Columbia, Vancouver, British Columbia, Canada, V6K 1Z4

*Author for correspondence (e-mail: gosline@zoology.ubc.ca)

Accepted 5 April 2008

SUMMARY

The silk that orb-weaving spiders produce for use as dragline and for the frame of the web is spun from the major ampullate (MA) glands, and it is renowned for its exceptional toughness. The fibroins that make up MA silk have previously been organized into two major groupings, spidroin-1 and spidroin-2, based largely on differences in amino acid sequence. The most apparent difference between spidroin-1 and spidroin-2 fibroins is the lack of proline in spidroin-1. The MA silk of *Araneus diadematus* comprises two spidroin-2 fibroins, and is therefore proline-rich, whereas spidroin-1 is preferentially expressed in *Nephila clavipes* MA silk, and so this silk is proline deficient. Together, these two silks provide a system for testing the consequences of proline-rich and proline-deficient fibroin networks. This study measures the mechanical and optical properties of dry and hydrated *Araneus* and *Nephila* MA silks. Since proline acts to disrupt secondary structure, it is hypothesized that the fibroin network of *Araneus* MA silk will contain less secondary structure than the network of *Nephila* MA silk. Mechanical and optical studies clearly support this hypothesis. Although the dry properties of these two silks are indistinguishable, there are large differences between the hydrated silks. *Nephila* silk does not swell upon hydration to the same degree as *Araneus* silk. In addition, upon hydration, *Nephila* MA silk retains more of its initial dry stiffness, and retains more molecular order, as indicated by birefringence measurements.

INTRODUCTION

Spider MA (major ampullate) silk is of great interest to researchers because of its unique properties of high strength and toughness. These unique properties have generated an interest in quantifying the mechanical properties of a variety of silks with the idea that silks can become commercially useful, or at least provide insight into novel ways of producing high strength superfibres. This may be accomplished by studying how processing the silk, amino acid sequence and protein secondary structure combine to produce the variety of properties seen among different silks.

MA silk is a strong material with a failure stress (~1 GPa) comparable to that of high tensile steel (Gosline et al., 1999) or to the aramid fibre, Kevlar (Hayashi and Lewis, 1998). Unlike these materials, MA silk is also highly extensible, with a failure strain of about 0.30. This combination of high strength and extensibility confers a degree of toughness unmatched by industrially produced materials. The molecular mechanisms that result in these remarkable properties have remained elusive. Understanding the relationship between amino acid sequence, protein secondary structure, fibroin network structure and the mechanical properties of MA silk in its functional states could lead to insights into how these remarkable properties are achieved.

In the web, MA silk functions in both the dry and the hydrated states. In the dry state, MA silk is much stiffer than most elastomeric proteins; however, it is worth noting that these proteins also function in the hydrated state. A more apt comparison would be between elastomeric proteins and MA silk in the hydrated state. Work (Work, 1977) found that when immersed in water, MA silk supercontracts, shrinking in length and increasing in volume. Supercontraction is associated with a change in mechanical properties and a decrease in birefringence (Work, 1977). The mechanics of supercontraction have been documented for the MA silk from a variety of spider species (Work, 1977; Work, 1981; Work, 1982; Work, 1985; Fornes et al., 1983). Birefringence studies have been used as a measure of molecular order within dry and supercontracted fibres and associated with the mechanical properties of MA silk. In these studies higher birefringence (higher molecular order) values are associated with stiffer, stronger fibres. The function of supercontraction is unknown; however, since the web is tethered to rigid structures, and MA silk is laid down in tension, supercontraction generates stresses of about 50 MPa (Savage et al., 2004; Work and Young, 1987) that could act to help tension the web.

At present, partial sequences are available for 21 fibroins expressed in the MA glands of ten species of spiders from six genera (Gatesy et al., 2001). In each case, the structure of the MA proteins is highly conserved, consisting of two distinct and repeated sequence blocks: (1) a poly-alanine block, 5–10 amino acids long and (2) a glycine-rich sequence block of about 20–30 amino acids long. MA silk fibroins have been grouped as either MA spidroin-1 or MA spidroin-2 according to the variation and frequency of stable repeating amino acid motifs within the glycine-rich sequence blocks. These motifs include GA, GGX and $GPG(X)_n$, where X represents a small subset of amino acids.

The most apparent difference between spidroin-1 and 2 is that spidroin-1 fibroins are deficient in the amino acid proline and spidroin-2 fibroins are proline rich. Thus, spidroin-1 and 2 probably have different propensities for secondary structure based on this difference in proline content. Molecular dynamics simulations of model peptides indicate that only those sequences containing proline exhibit elastin-like properties, and only sequences devoid of proline had a propensity to aggregate into amyloid-like fibrils (Rauscher et

Fig. 1. The consensus sequences for the fibroins expressed in the MA glands of *Nephila clavipes* and *Araneus diadematus,* as presented in Gatsey et al. (Gatsey et al., 2001). Nc-MA-1 is spidroin-1 type and Nc-MA-2 is spidroin-2 type. Ad-MA-1 and Ad-MA-2 are both spidroin-2 type and were previously called ADF-3 and ADF-4 by Guerette et al. (Guerette et al., 1996). The percentage values at the end of each sequence give the relative size of the poly-alanine block and the percentage proline in each consensus repeat.

al., 2006). Indeed, an analysis of the proline and glycine content of elastomeric proteins and amyloids indicate that elastin-like behaviour occurs above a threshold level of combined proline and glycine content (Rauscher et al., 2006). That study identified proline as the primary determinant of elastin-like behaviour, and noted that spidroin-1 fibroins are below the proline and glycine threshold, and so are likely amyloidogenic, whereas spidroin-2 fibroins are above the threshold, and hence should be elastin-like.

Araneus diadematus MA glands are unique amongst those studied thus far, in expressing two spidroin-2 type genes, *Ad-MA-1 and Ad-MA-2* (Fig. 1) (Guerette et al., 1996). Gatsey et al. (Gatsey et al., 2001) classified a third fibroin (ADF-2 isolated by Guerette et al.) as a MA-spidroin-1 type fibroin, but this fibroin was isolated from a cDNA library derived from the cylindrical gland, which produces cocoon silk. Using northern analysis ADF-2 was found to be expressed in the cylindrical gland and was below detection limits in the MA gland. Thus, the predominant fibroins expressed in the *Araneus* MA gland are elastin-like and contain about 16% proline, and the MA gland contains about 16% proline (Andersen, 1970). The *Araneus* fibroins are, at first glance, analogous in structure to elastin, containing both a poly-alanine sequence block and a glycine and proline-rich sequence block. *Nephila clavipes,* however, expresses one gene from each group, *Nc-MA-1*, encoding a spidroin-1 fibroin, and *Nc-MA-2* encoding the elastin-like spidroin-2 fibroin (Fig. 1). Since the *Nephila* MA gland contains approximately 3.5% proline (Work and Young, 1987) and the Nc-MA-2 gene product contains about 18% proline, we estimate that Nc-MA-1 makes up about 80% of the content of the gland.

Studies into the structure of spider silks have focused mainly on the MA silks because of the requirement of large samples to obtain diffraction patterns with X-ray crystallography. X-ray diffraction of MA silks has revealed an ordered phase of anti-parallel β-sheet crystals embedded in a softer, or 'amorphous' phase (Warwicker, 1960). A more detailed analysis of the ordered phase has revealed an inter-sheet spacing of 0.53–0.55 nm for several spider species within the *Araneus* and *Nephila* genera (Becker et al., 1994; Grubb and Jelinski, 1997; Sheu et al., 2004; Warwicker, 1960; Work, 1982). This spacing is consistent with that found in β-sheet crystals of poly-alanine or alanine alternated with glycine or serine (Fraser and MacRae, 1973). Grubb and Jelinski (Grubb and Jelinski, 1997) reported the mean crystal dimensions to be 2 nm×5 nm×7 nm, a size consistent with the scale of the poly-alanine blocks found in the fibroins discovered to-date.

These crystals have been shown to be strongly aligned with the fibre axis and to occupy about 10–15% of the total volume of the fibre (Fornes et al., 1983; Grubb and Jelinski, 1997; Yang et al., 1997). These conclusions have been subsequently confirmed by nuclear magnetic resonance (NMR) (Simmons et al., 1996; Kummerlen et al., 1996) and Raman spectroscopy studies (Shoa et al., 1999; Edwards et al., 1995). The study by Simmons et al. (Simmons et al., 1996) found that in addition to the highly oriented β-sheet crystals, a second population of alanine residues existed as weakly orientated, unaggregated β-sheet. In fact, 40% of the alanine present existed as highly oriented β-sheet while the remaining 60% existed as the more poorly aggregated β-sheet, implying that the crystal volume fraction is actually 20–25%, a value higher than that presented by X-ray crystallography. X-ray diffraction of bundles of MA silk (Grubb and Jelinski, 1997) and of single fibres (Riekel et al., 1999) has confirmed the presence of two populations of β-sheets.

Since supercontracted *Araneus* MA silk behaves like a filled rubber (Gosline et al., 1984), and exhibits rubber-like elasticity, the theory of rubber elasticity can be used to develop a model of fibroin network structure. The application of this model requires two major assumptions: (1) that the individual fibroin molecules are crosslinked to form a mechanically continuous fibroin network, and (2) the fibroin network chains between crosslinks adopt an amorphous, kinetically free, random-coil state. When this random-coil network is stretched, the conformational entropy of the network chains falls, and this change in entropy provides the rubber-like, entropic elastic mechanism. The modelling process is based on the increasing stiffness of the network as the amorphous random-coil network chains are straightened. This increase in stiffness associated with straightening network chains of finite length is compared to the Gaussian ideal of network chains of infinite length. The rise in stiffness of the fibroin network from the Gaussian ideal reveals information as to the length and stiffness of the network chains. Such analysis predicts network chains of 15–20 amino acids with a length of 8–10 amino acids required for the chain to behave as a single 'ideal' link in the random chain (Gosline et al., 1994). Thus, the model predicts network chains that are 10–15 amino acids shorter than the elastin-like network chains found in the spidroin-2 fibroins expressed in *Araneus*. However, the model predicts the length of network chains based on the assumption that all bonds in the peptide backbone have equal rotational freedom. If this is not the case, the model will underestimate the number of amino acids in the network chains.

Using the same assumptions of the two-phase model, Termonia (Termonia, 1994) created a three-phase molecular model that accurately predicted the mechanical properties of both wet and dry MA silk. This model has the added refinement that the network chains leaving the crystals are constrained and have a higher stiffness than that in the bulk of the network chains. This restriction on the mobility of network chains may account for the difference in the length of network chains seen in the *Araneus* fibroins and the length of network chains predicted by the network model described above. The model prediction that network chains are shorter than those indicated by sequence data indicates that five to seven amino acids are required to relieve the constraining effect of the crystals before the network chains are fully able to adopt amorphous conformations. The actual sequence data for the Araneus fibroins (Fig. 1) indicate that proline occurs within two to five residues on either end of the poly-alanine sequence blocks. Thus, the conformational 'kink' imposed by proline should disrupt the structure of the network chains

as they emerge from the poly-alanine β-sheet crystals. This will make more of the network chains available to adopt amorphous conformations.

Although fibroin network models for *Araneus* MA silk assume amorphous network chains, physical studies based on X-ray diffraction and NMR have provided alternative hypotheses for the structure of the network chains in other MA silks. In the case of *Nephila*, spidroin-1 (Fig. 1; Nc-MA-1) is preferentially expressed, and the lack of proline means that the majority of the network chains will be highly constrained as they exit the poly-alanine β-sheet crystals, and this could facilitate the transition to stable secondary structures. Thiel et al. (Thiel et al., 1997) proposed a model for *Nephila* MA silk, which stated that the poly-alanine regions would form the β-sheet crystals, and the glycine-rich sequence blocks would also form a non-periodic crystal lattice with varying degrees of perfection depending on their ability to associate with their nearest neighbours. A helical conformation has also been proposed as the stable secondary structure for the network chains, based on NMR of *Nephila* MA silk (Kummerlen et al., 1996). This study found the best fit to be axially aligned, 3_1 helices stabilized by inter-chain hydrogen bonding. The stiffness and high strength of MA silks was attributed to this inter-chain hydrogen bonding. van Beek et al. (van Beek et al., 2002) proposed a hierarchical model of silk structure in which fibrillar substructures make a core that is covered by a hard skin, or outer core. In turn the fibrillar substructures are composed of a network in which β-sheet crystallites reinforce a network of 3_1 helices (van Beek et al., 2002). An NMR study on dry, hydrated, restrained and supercontracted *Nephila* MA silk also showed local structure in the dry state, possibly 3_1 helices (Eles and Michal, 2004a).

To date, fibroin network models have been based on mechanical data from *Araneus diadematus,* and proposed secondary structures have been based on X-ray or NMR of *Nephila* species. The presence of stable secondary structure in *Nephila* means that current network models of *Araneus* might not apply to *Nephila*. However, if the secondary structure is not stable and 'melts' with hydration, as suggested by NMR data, a 'latent' rubber-like mechanism may also exist in this silk (Eles and Michal, 2004b). The validity of a rubber-like model for *Nephila* silk would then depend on the propensity of hydrated network chains to re-form the stable secondary structures seen in the dry state, as the silk is extended. Mechanical tests on hydrated *Nephila* silk may provide insight into the validity of a rubber-like elastic mechanism.

Thus, *Araneus* and *Nephila* MA silks provide a system for testing the consequences of having a proline-deficient network *versus* a proline-rich network on the properties of MA silks. This is based on the ability of the network to form strong, stable hydrogen bonds depending on the propensity of the network chains to form secondary structures. Fig. 2 is a conceptual model depicting hypothetical distributions of bond energies, or bond strengths, of the hydrogen bonds contained within either proline-rich (+Pro) or proline-deficient (–Pro) networks. In both cases the network is held together by poly-alanine β-sheet crystal crosslinks. The regular repeating pattern within the poly-alanine crystals provides the ideal bond length and angles for hydrogen bonding, and consequently the hydrogen bonds are strong and stable, even in the presence of a polar solvent such as water. Conversely, the peak representing the distribution of bond energies within the proline-rich network chains is broader and is shifted left to lower energy levels. This indicates that, while extended during silk spinning, the network chains are essentially random-coils that have been aligned to the fibre axis and stabilized by hydrogen bonds, and are therefore well below their glass transition temperature, *Tg*. Since there is no particular secondary structure to these straightened random-coils, the hydrogen bonds are not necessarily at an ideal length or angle and thus are at lower energy levels than those in the stable, regular poly-alanine crystals.

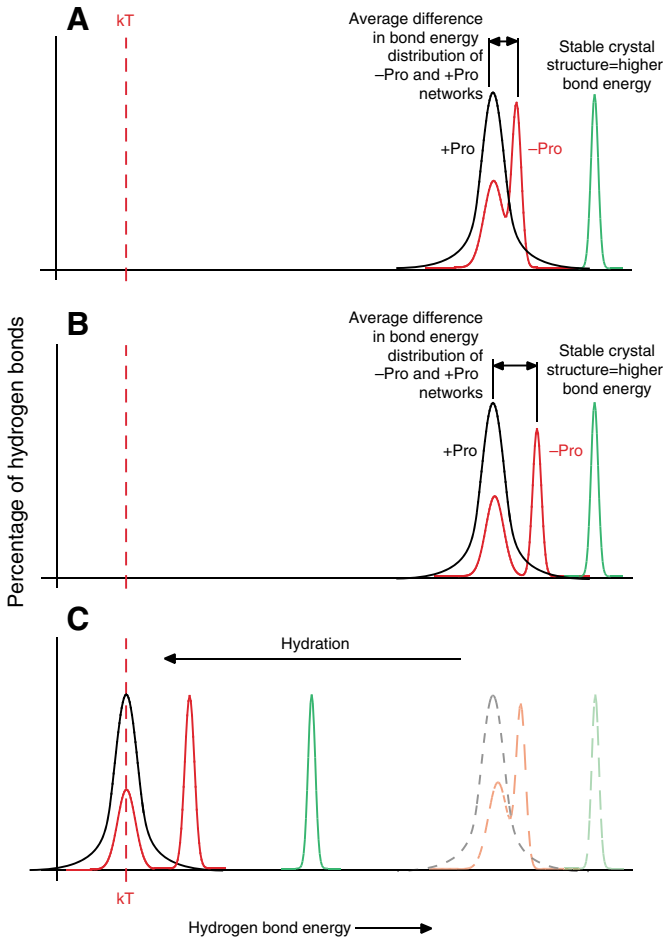

Fig. 2. A conceptual model representing the distribution of hydrogen bond energies contained within proline-rich (+Pro) *Araneus* and proline-deficient (–Pro) *Nephila* MA silk networks. Green peaks represent bond energies in poly-alanine β-sheet crystals; black peaks represent bond energies in the network chains in *Araneus* silk, and red peaks represent bond energies in the network chains in *Nephila* MA silk. (A,B) Two possible scenarios for the bond energy distributions of the silks in the dry state. In A the distribution of hydrogen bond energies in +Pro and –Pro networks are not sufficiently different to be detected in the dry mechanics. In B the difference in hydrogen bond energies between +Pro and –Pro networks is sufficiently large that there are significant differences in the dry mechanics. According to both dry models, the peaks associated with hydrogen-bonded structures are well above the energy associated with Brownian motion, kT, and thus represent stable structures. (C) Hydration weakens the hydrogen bond strengths of the +Pro networks, and consequently the +Pro peak shifts to levels that are near or below kT. It is unclear where on this scale the –Pro peak might shift; however, if it remains above kT, we hypothesize that there would be a difference in the properties of hydrated MA silks. The poly-alanine β-sheet crystals are stable both in the dry and hydrated state, and it is unclear if the crystals 'soften' in the presence of water. We arbitrarily shifted the poly-alanine peak to the left slightly, but the position well to the right of kT indicates that the poly-alanine crystals are quite stable in water.

The distribution of bond energies within the proline-deficient network is represented by a bimodal distribution. This means that even in the proline-deficient network, not all the chains have a

secondary structure as regular and as stable as the poly-alanine β-sheet crystals. A small population of hydrogen bonds is at the bond energy associated with the proline-rich network, but the majority of bonds are associated with the secondary structures proposed to exist within the proline-deficient network chains of *Nephila* silk. These hydrogen bonds are at higher energy levels and fall somewhere between that proline-rich peak and the peak representing the poly-alanine crystals. Of course, exactly where the proline-deficient peak falls between the proline-rich peak and the poly-alanine peak is unknown. If the distributions of hydrogen bond strength were similar between the proline-rich and proline-deficient networks, as is depicted in Fig. 2A, then we would expect the dry mechanics of *Araneus* and *Nephila* MA silks to be similar. However, if the secondary structures associated with the proline-deficient network chains are particularly stable, there may be a significant difference in the bond strength between proline-rich and proline-deficient networks (Fig. 2B). If this were the case, then we would expect a measurable difference in the mechanical properties of dry MA silks.

Dry MA silks can be considered as composite-like materials consisting of strong, stiff poly-alanine crystal crosslinks that reinforce a softer, glycine-rich matrix. The initial modulus of the silk is a result of the crystals and the matrix acting in series. If the matrix is stiffer because of the strength of the stabilizing hydrogen bonds, then the initial modulus will be higher. The yield points represent the strain at which stress is sufficiently high to break the hydrogen bonds, allowing the network chains to be extended. Thus, if there were significant differences in the bond energy distributions between proline-rich and proline-deficient networks, we would specifically predict measurable differences in the yield points and in the initial modulus.

Fig. 2C shows the effect of hydration on hydrogen bond energies within MA silk networks. In both cases, it is known that the poly-alanine β-sheet crystals are relatively unaffected by water (Work, 1982), and so this peak remains well away from kT (the energy associated with Brownian motion) upon hydration. Of course, it is unknown if the poly-alanine β-sheet crystals are completely unaffected by water, or if the crystals soften, becoming less rigid upon supercontraction. In Fig. 2C we have chosen, somewhat arbitrarily, to shift the poly-alanine peak to a lower stability upon supercontraction, but it remains well away from kT, as these crystals clearly do not 'melt' in water. Based on thermoelastic experiments on hydrated *Araneus* MA silk (Gosline et al., 1984), we know that a hydrated, proline-rich network becomes rubber-like, exhibiting entropic elasticity. Consequently, the proline-rich peak has been shifted to a lower energy, at or near kT. Thus, the hydrogen bonds within the network chains are easily broken and reformed, and the network chains behave, on average, as kinetically free, random-coils. Likewise, one would expect the same shift in bond energy for those portions of the proline-deficient network not contained within stable secondary structure. However, it is not clear where on this spectrum the peak representing proline-deficient secondary structure will fall. Yet, if the peak falls anywhere on the scale above kT, as indicated in Fig. 2C, then even if hydrated, the proline-deficient network chains will maintain some secondary structure. If this is the case, then we expect there to be measurable differences in the mechanical properties of the hydrated MA silks. Specifically, the proline-deficient network (*Nephila*) will not shorten and swell as much as the proline-rich MA silk (*Araneus*). In addition, the hydrated *Nephila* MA silk will remain stiffer and contain more ordered structures as indicated by birefringence measurements.

Studies on spider silks are difficult because of the small diameter of the fibres, and some variability exists in the literature depending on the criteria used to define diameters by individual researchers. This study quantifies supercontraction properties, wet and dry mechanical data, and wet and dry birefringence values for *Araneus* and *Nephila* MA silk. The same researcher using the same criteria for difficult measurements such as diameter and birefringence produced the data provided here. Based on the physical data reviewed above for *Araneus* and *Nephila* MA silk, it is hypothesized that there will be significant differences in the mechanical and optical properties of these two silks. The results clearly confirm this prediction.

MATERIALS AND METHODS

Adult female *Araneus diadematus* (Clerck 1757) spiders were collected locally, in the University Endowment Lands of the University of British Columbia, and *Nephila clavipes* (Linnaeus 1767) were collected in Gainesville, FL, USA. Spiders were maintained in the lab in 50 cm×50 cm×15 cm cages, as described previously (Witt, 1971), were fed and given water regularly, and were producing normal webs. Silk was collected by allowing the spiders to roam freely over a level, black surface. The MA silk left behind as a safety line was carefully collected onto paper frames cut from 10 cm×15 cm recipe cards so that it remained at its natural length. Each sample used in the experiments was from a different individual spider.

Supercontraction properties

When submersed in water, MA silk supercontracts, shrinking in length and increasing in cross sectional area. Length contraction was measured by placing an approximately 3 cm long piece of dry silk fibre on a moveable micrometer mount described below. The micrometer was moved under ×50 magnification until the slack in the fibre was just taken up. Water was then added and the micrometer was moved until the slack in the wetted fibre was just taken up. The wet to dry ratio was the ratio of the wet and dry lengths as measured to the nearest 0.05 mm by a pair of vernier calipers.

The ratio of wet to dry diameter was measured under a ×100 oil immersion lens on a Leitz Orthoplan polarizing microscope using a ×15 filar micrometer eyepiece, for a total magnification of ×1500. The system was calibrated using a 10 μm calibration slide (Bausch and Lomb, Rochester, NY, USA). Dry fibres were mounted with the slack taken up on a slide, placed in immersion oil, covered with a cover slip and observed through immersion oil. For supercontracted diameters, fibres were mounted as dry fibres then wetted, and one end was cut allowing the fibre to recoil. The fibre was then covered with a cover slip and observed through immersion oil.

Mechanical testing

The mechanics of dry dragline silk were tested on an Instron (Norwood, MA, USA) universal testing machine (model 5500) with a custom built load cell that could be used at a sensitivity of 1 g force full-scale. Silk was fastened to a 13 cm×26 cm card with the centre cut out to produce a frame. The specimen was fastened to the frame by Scotch 810D 'Magic Tape' and the free ends were glued down with Devcon five minute epoxy. Once the card was fastened to the Instron by means of two screw-tightened clips, the sides of the frame were cut away. The crosshead was moved to adjust the length so the silk was just slack. The crosshead speed was 10 mm min^{-1}, which for samples of approximately 5 cm gave a strain rate of approximately 20% per minute (0.003 s^{-1}).

Supercontracted silk was stretched under equilibrium conditions on a microscope-based, glass micro-beam test apparatus, which has been previously described (Gosline et al., 1995; Fudge et al., 2003; Savage et al., 2004). A video dimension analyzer (VDA) tracked the movement of the glass beam, and this movement was translated into force. In order to obtain stress, the cross-sectional area of the silk was determined on the test frame by measuring the diameter of the silk using a ×20, polarizing objective and a ×15 filar micrometer eyepiece for a total magnification of ×300.

Material properties were calculated by converting force into engineering stress (σ) based on initial cross-sectional area ($\sigma=F/A_0$; where F is force and A is the initial cross-sectional area of the silk fibre), and deformation was converted into engineering strain ($\epsilon=\Delta L/L_0$; where ΔL is the change in fibre length and L_0 is the initial fibres length). In all cases, the initial dimensions (A_0 and L_0) correspond to the dimensions of the silk samples in their dry or wet states, as appropriate.

Birefringence measurements

Birefringence measurements were taken on dry, wetted but restrained, and supercontracted dragline fibres using a Wild M-21 polarizing microscope. Dry fibres were mounted in oil and measured with a ×40 objective, a ×1.25 extension, and a ×15 filar micrometer eyepiece for a total magnification of ×750. Wet, restrained fibres were measured with the same magnification setup but under water.

The birefringence of supercontracted dragline was measured when at slack length and at two to four percent increments of strain. The apparatus used for strain measurements of supercontracted fibres was similar to that used for mechanical tests, with the exception of a stationary mount instead of the glass micro-beam. The thickness of this device prevented the use of high magnification. As a consequence diameter measurements were taken at a magnification of ×300. All birefringence measurements were taken using a Wild Senarmont 546 nm compensator with a 546 nm interference filter. The specimen was placed at 45° to crossed polarizers (point of maximum brightness), and the analyzer was rotated until the specimen reached extinction. The retardation, Γ, caused by the sample is equal to 3.03 nm multiplied by the analyzer angle in degrees. The path length was measured as the diameter, d, of the fibre taken at or near the location of the birefringence reading, and the birefringence, $B=\Gamma/d$.

RESULTS

Dry mechanics

Fig. 3 shows a typical stress *vs* strain trace for dry MA silks from *Araneus* and *Nephila*. Mean values from the dry mechanical data are shown in Table 1. The standard deviation of each mean is included to represent the natural variability of individual fibres. The properties of these two MA silks are very similar; both have an initial modulus, E_o, of about 10 GPa and a failure stress, σ_f, of about 1 GPa, which is consistent with values published for *Araneus sericatus* (Denny, 1976). Neither the mean E_o nor mean σ_f were statistically different based on a Student's t-test (E_o: t-statistic=–1.199, P=0.238; σ_f: t-statistic=0.445, P=0.659). The yield stress for *Araneus* and *Nephila* MA silks were σ_y=157 MPa and σ_y=174 MPa, respectively, and they were not statistically different (Mann–Whitney rank sum test, T=209, P=0.1). The yield strain for *Araneus* and *Nephila* MA silks were ϵ_y=0.017 and 0.019, respectively, and were not statistically different (t-statistic=–1.170, P=0.251).

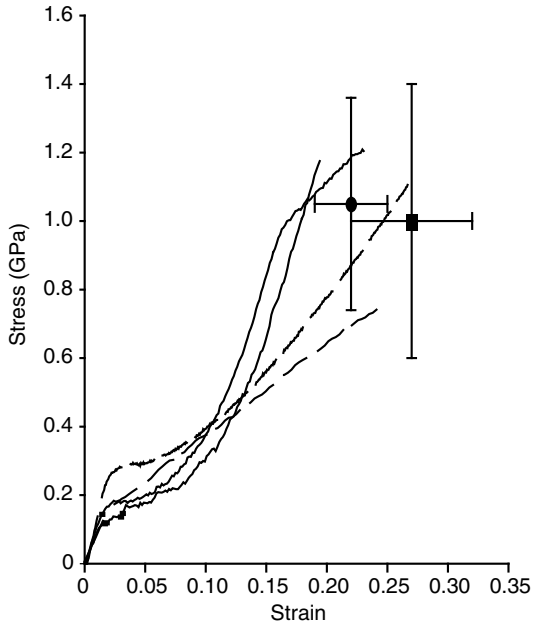

Fig. 3. Typical tensile test data for dry MA silk collected from *Araneus* and *Nephila*. Traces were chosen to demonstrate the range of data collected. Dashed traces are data from *Nephila*, unbroken traces are data from *A. diadematus*. The black circle represents the mean failure stress and strain for *Araneus* with error bars representing one standard deviation. The black square represents the same values for *Nephila*. Each sample was from a different spider.

The failure strain of *Nephila* MA silk is 0.27, similar to that published previously for *Nephila* (Cunnliff et al., 1994) and also similar to the failure strain for *Araneus sericatus* (Denny, 1976). The failure strain of *Araneus* MA silk was ϵ_f=0.23, which is the same as the value reported for *Araneus gemmoides* (Stauffer et al., 1994) and within the range of values reported for *Araneus sericatus* (Denny, 1976). However, the failure strain of *Nephila* MA silk was statistically higher than the failure strain of *Araneus* MA silk (t-statistic=–3.607, P=0.001), although the difference is quite small.

Hydrated mechanics

Table 2 summarizes the parameters of supercontraction for *Araneus* and *Nephila* MA silk. *Araneus* contracts in length by about 50% and increases in cross-sectional area by almost a factor of 5, for a total volume-swelling ratio from wet to dry of 2.42. This is higher than the swelling of *Nephila* MA silk, which shrinks in length by 34% and increases in cross-sectional area by 2.56 times, for a total

Table 1. Mean values for initial modulus, breaking stress and strain for dry MA silk fibres

	Initial modulus (GPa)	Yield, strain	Yield, stress (MPa)	Final modulus (GPa)	Failure, strain	Failure, stress (GPa)
Nephila clavipes (*N*=17)	10.98±4.45	0.019±0.003	170.7±34.8	3.26±1.04 (*N*=16)	0.27±0.05*	0.79±0.29
Araneus diadematus (*N*=18)	10.10±4.28	0.017±0.004	157.4±76.7	4.11±2.49	0.22±0.03*	1.05±0.31

The errors represent ±1 standard deviation. *A statistical difference (P=0.001).

Table 2. Supercontraction length ratios and swelling data for MA silk of *Araneus diadematus* and *Nephila clavipes*

	A. diadematus (*N*=12)	*N. clavipes* (*N*=12)
Length contraction ratio (wet/dry)	0.50±0.02	0.66±0.03
Wet/dry cross-sectional area	4.83±0.25	2.56±0.11
Volume ratio (wet/dry)	2.42	1.69

The errors represent ± 1 standard error. Differences are statistically significant at $P<0.05$.

volume-swelling ratio of 1.69. Our values for *Araneus* MA silk can be compared to data acquired by Work (Work, 1977), who recorded a wet to dry length ratio of 0.55 and a wet to dry cross-sectional area ratio of 3.90 for dragline silk samples. Our length contraction ratio is quite similar, but our cross-sectional area ratio is about 25% higher. This seems acceptable given the difficulty in obtaining diameter measurements from such small fibres.

The mechanical properties of supercontracted MA silks are shown in Figs 4, 5 and 6. Fig. 4A shows individual test results from 12 samples of *Araneus* MA silk, and Fig. 5A shows individual test results from 24 samples of *Nephila* MA silk. Since the data exhibit a high degree of variation, an averaged curve has been generated for each data set and is shown in Fig. 4B and Fig. 5B for *Araneus* and *Nephila*, respectively. Each individual test in the *Araneus* data set was fitted to a second or third order polynomial, and the *Nephila* data were fitted to either a third or fourth order polynomial. The equations were solved at 5% increments as explained below. Since the individual samples were not tested to failure, but rather to the largest strain allowed by the experimental setup, each equation was solved only to the largest strain achieved for that respective test. The predicted values at each 5% increment were averaged from every curve for which a value was available and plotted with standard deviations. For the purposes of direct comparison, the data for *Araneus* and *Nephila* are shown together in Fig. 6. There is a large degree of variation within both data sets; however, there is clearly minimal overlap between the two data sets, indicating that supercontracted *Nephila* MA silk is initially much stiffer than *Araneus* silk.

Fig. 7 shows how the stiffness of *Araneus* and *Nephila* MA silk increases with strain, and these lines are obtained by taking the first derivative of the regression lines in Fig. 4B and Fig. 5B. The data derived from the regression analysis for *Araneus* MA silk exhibited a nearly tenfold increase in the stiffness by a strain of 0.1. Since none of the individual tests (Fig. 4A) exhibited such a large increase in stiffness at low strains, it was assumed that the average MA silk properties derived from the regression analysis did not accurately portray the silk behaviour at low strains. Thus, in Fig. 7, the modulus data are plotted between the strains of 0.1 and 0.65. In order to clarify the shape of the stiffness curves in Fig. 7, the average of initial modulus values taken from the individual mechanical tests are also plotted for *Araneus* and *Nephila* MA silk at zero strain, with error bars that indicate one standard error of the mean. Fig. 7B plots the data from Fig. 7A on a log scale and clearly shows the difference in stiffness between *Nephila* and *Araneus* silks with increasing extension.

The average initial stiffness calculated from the mechanical tests of hydrated *Araneus* and *Nephila* MA silk is 10.0±1.9 MPa and 97.4±34.6 MPa, respectively, a tenfold difference. These experiments show a drop in initial stiffness from that of the dry state of 1010-fold for *Araneus* and 113-fold for *Nephila*. Clearly, *Nephila* MA silk retains much more of its initial, dry stiffness upon supercontraction; however, it is interesting to note that, with increasing extension, the stiffness of hydrated *Araneus* MA silk begins to approach that of the *Nephila*. Indeed, by a strain of 0.65, the *Nephila* MA silk is only about 1.7 times stiffer than *Araneus* MA silk.

Birefringence

Birefringence data is shown in Figs 8–10 and Table 3. Table 3 shows the effect of hydration on the birefringence of silk fibres. Birefringence values are clearly higher for *Nephila* in all experiments: dry, wetted/restrained, supercontracted and supercontracted with strain. Values for *Araneus* are generally lower than those reported by Work (Work, 1977); however, the trends are the same, birefringence being highest for dry fibres and lowest for supercontracted fibres. In each case, for *Araneus* and *Nephila* MA silk the trends in birefringence shown in Table 3 are the same; however, the magnitude of the changes from dry to supercontracted

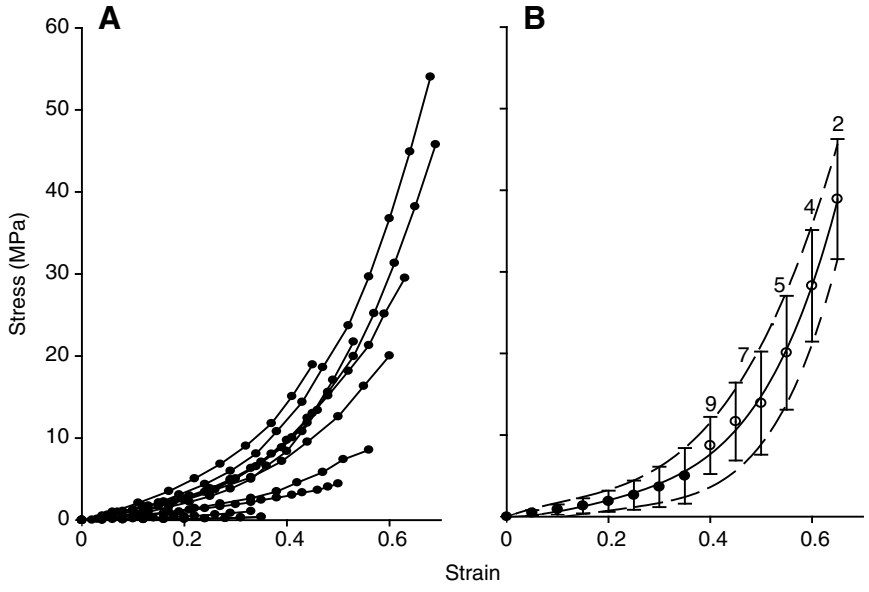

Fig. 4. Supercontracted properties of *Araneus* MA silk. Note that the individual samples were not tested to failure, but to the highest strain possible with each experimental setup. (A) The complete data set; (B) the average behaviour of the data set. Predicted values were averaged from all the curves for which a value was available. Filled circles represent values averaged from all 12 tests and open circles represent values averaged from all tests for which a value at that extension was available. The numbers above each data point are the number of curves included in the average. The calculated average behaviour is fitted to the fourth order polynomial, $450.05x^4-310.64x^3+109.49x^2-4.29x+0.22$, $r^2=1$. Error bars are one standard deviation. Each sample was from a different spider.

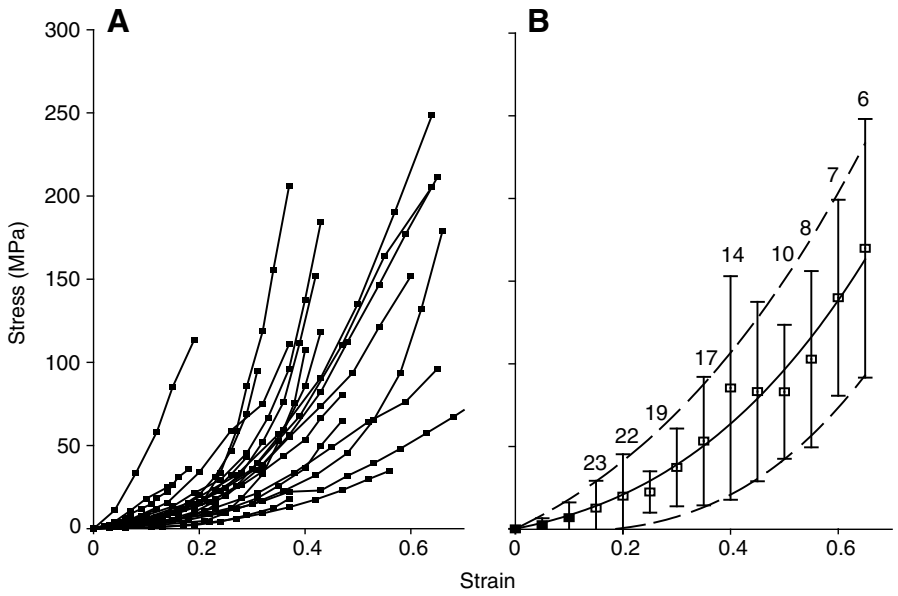

Fig. 5. Supercontracted properties of *Nephila* MA silk. Note that the individual samples were not tested to failure, but to the highest strain possible with each experimental setup. (A) The completed data set; (B) the average behaviour of the data set. Predicted values were averaged from all the curves for which a value was available. Filled squares represent values averaged from all 24 tests and open squares represent values averaged from all tests for which a value at that extension was available. The numbers above each data point are the number of curves included in the average. The calculated average curve is fitted to a third order polynomial, $266.23x^3+81.42x^2+89.11x-2.21$, $r^2=0.97$. Error bars are one standard deviation. Each sample was from a different spider.

are larger for the *Araneus* MA silk. The birefringence of both silks falls by roughly 10–15% when hydrated but restrained; however, when supercontracted the birefringence falls by a factor of four in *Araneus* but only by a factor of about two in *Nephila*.

This difference is reflected in the birefringence-strain behaviour of these two silks. Fig. 8A shows individual test results from nine samples of hydrated *Araneus* MA silk. The individual samples show a high degree of variability; however, the average initial slope of the nine birefringence-strain tests is 0.0122. Fig. 9A shows individual test results from seven tests of hydrated *Nephila* MA silk.

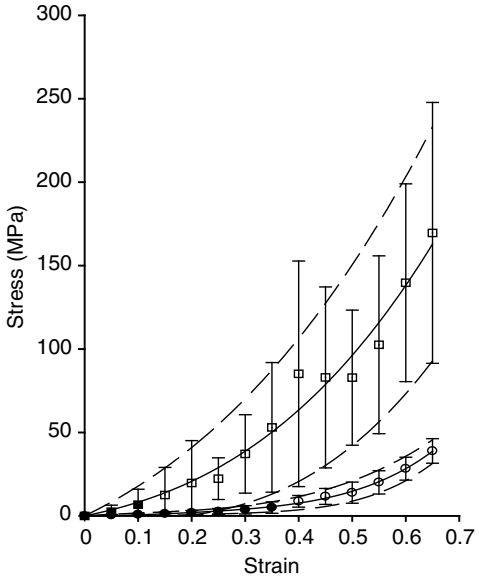

Fig. 6. The average stress–strain behaviour presented in Fig. 4B (*Araneus*) and Fig. 5B (*Nephila*) are presented on the same axis for the purposes of direct comparison. Squares represent *Nephila* MA silk and circles represent *Araneus* MA silk. As for Figs 4 and 5, filled symbols represent values from all tests for which a value was available, and open symbols represent values from all tests that were available at that extension. The average *Nephila* MA silk behaviour is stiffer and the stress rises more quickly with increasing extension than is the case with *Araneus* MA silk.

Again, the individual tests show a high degree of variability, but the average slope of all the tests is 0.0456. Thus, *Nephila* MA silk has approximately three times the birefringence of *Araneus* silk when just slack, and in addition, the birefringence readings increase with increasing strain, and the slope is four times higher in *Nephila* than is in *Araneus*. Because of the high degree of variability in both data sets, an averaged curve has been generated as above (using second or third order polynomials) for both *Araneus* and *Nephila* (Fig. 8B and Fig. 9B, respectively). For the purposes of direct comparison, the data for *Araneus* and *Nephila* are shown together in Fig. 10, which clearly shows that there is no overlap between the two data sets.

DISCUSSION

Tests on the dry MA silks showed that *Araneus* and *Nephila* MA silks are virtually identical in all mechanical properties. Indeed, only failure strain showed a significant difference, and this difference was quite small (Fig. 3; Table 1). Perhaps this is not surprising because for both silks in the dry state the network chains have little mobility, and the materials can be considered as rigid, polymeric solids. Both silks contain fibroins that have essentially the same length of poly-alanine sequence blocks (Fig. 1), and there are similar amounts of β-sheet crystals in the spun fibres. In addition, both have similar lengths of glycine-rich network chains, which in the dry state are likely to be rigid due to the absence of water or other plasticizing solvents. In *Nephila* there is strong evidence of ordered structure in the network chains, and in *Araneus* the dry network chains have been described as polymeric glass (Gosline et al., 1984). Thus, it is tempting to conclude from the dry mechanical properties that there is no difference in the strength of the hydrogen bonds that stabilize the network chains in these two dry MA silks.

It is unwise, however, to jump to this conclusion, because the exceptional variability of spider silks may simply have masked real differences that might exist if more uniform silk samples were tested. We now know that spiders have a friction brake, located within the spinning apparatus, that they can use to apply a force to the silk threads as they are drawn from the spinneret. Spiders can control this force to levels that range from 0.1 to 4 times the spiders' body weight, and at its highest levels this force can create stresses in excess of 50% of the silk's tensile strength (Ortlepp and Gosline, 2004).

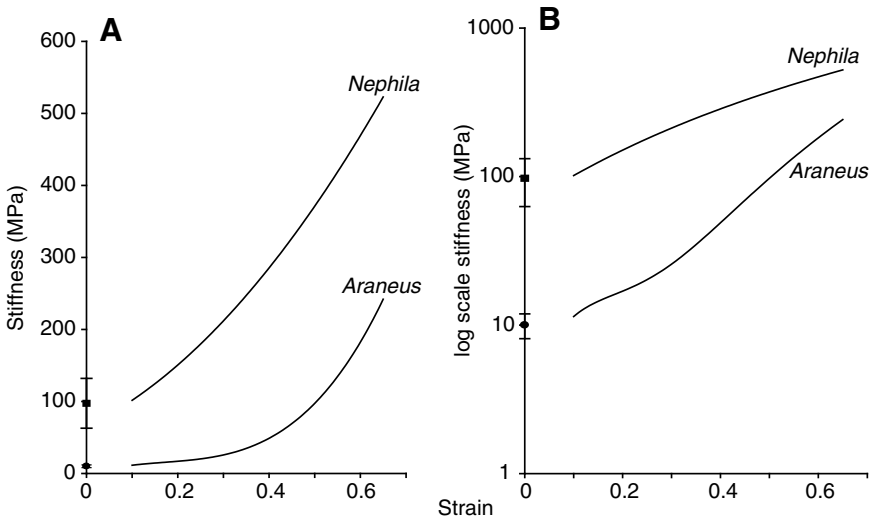

Fig. 7. (A) The instantaneous modulus of MA silk is plotted against strain. The *Araneus* curve is difficult to distinguish from the axis because of the relatively high modulus of *Nephila*. (B) To better distinguish the *Nephila* and *Araneus* curves, the data from A is plotted as log modulus *versus* strain. The solid squares indicate the initial stiffness of *Nephila* silk, and the solid circles indicate the initial stiffness of *Araneus* silk.

This friction brake, therefore, will have important implications for the amount of draw-induced alignment within the MA silk network and hence the properties of the silks formed. Indeed, Perez-Rigueiro et al. (Perez-Rigueiro et al., 2005) were able to measure the silking forces and the tensile properties of individual MA silk fibres, and they were able to show a strong correlation between the silking stress during spinning and the tensile properties of that silk. It was found that as the silking stress increased, the silk fibres became both stiffer and less extensible. This study also quantified a range of properties present in silk naturally spun by the spiders; presumably the large variability seen in naturally spun silk is a result of the spiders' ability to vary the force on the silk as it is produced. Since the silk samples used in this study were obtained from the draglines left by freely walking spiders, we do not know if the samples used were spun under the same conditions. Thus, it is possible that the lack of difference in dry mechanical properties is simply due to the variability of the samples used, which means that the dry data may not be sufficient to determine if there are differences in hydrogen bonding in the network chains of these two silks. The birefringence data for the dry silks may, however, provide a better indication of this difference.

Dry *Nephila* silk has roughly 50% higher birefringence than dry *Araneus* MA silk (Table 3, $P<0.001$), and since both silks have similar amounts of poly-alanine, β-sheet crystals, it is likely that there are real differences in the network structure of these two silks. Apparently the regular repeating pattern of bond angles within the protein backbone and the regular pattern of hydrogen bonding that can occur in the stable secondary structures of the network chains in *Nephila* MA silk create a molecular alignment that is greater than that created by the extension of the amorphous chains in *Araneus*. So it is still possible that there are significant differences in the strength of hydrogen bonding between these two silks in the dry state, even if sample variability prevented us from observing this in the dry mechanical tests. The supercontraction behaviour may help resolve this issue.

If the secondary structures in the proline-deficient network of *Nephila* MA silk do not 'melt' in water, it is an indication that water is not able to penetrate and disrupt the hydrogen bonds that stabilize these structures. Alternatively, if the hydrogen bonds in the proline-rich network of *Araneus* MA silk are disrupted by water, then these bonds must be weaker than those in *Nephila* silk, and the transition to the supercontracted state might be more dramatic for *Araneus* than *Nephila* silk. Our results show that this is indeed the case. *Araneus* MA silk swells to a much larger volume than *Nephila* silk, indicating that water is more able to penetrate the network of the *Araneus* silk. In addition, *Araneus* MA silk contracts to a shorter relative length upon hydration, suggesting that more of its structure 'melts' in water (Table 2). Presumably, the greater swelling and contraction seen for *Araneus* silk is due to the disruption of the hydrogen bonds that stabilize the extended glass structure of the network chains in *Araneus* silk, which collapse from the drawn state into an amorphous network when hydrated. *Nephila* apparently maintains some structure that does not 'melt', and the 34% decrease in length (Table 2) is probably due to the reorientation of large-scale structures. Thus, there appear to be clear differences in the stability of the hydrogen bonds that exist in the network chains of these two silks in their dry state. Comparison of the changes in birefringence with supercontraction provides additional insights into this process.

The data in Table 3 indicate that the birefringence of *Nephila* MA silk falls by about 50% when the silk is supercontracted in water, whereas *Araneus* MA silk's birefringence falls by 75%. As a result, the difference in birefringence of these two silks in their supercontracted states is approximately threefold. We interpret these changes as follows. Because the poly-alanine, β-sheet crystals in MA silks do not melt when these silks supercontract in water (Fornes et al., 1983), we know that the changes in birefringence arise from changes in the state of the network chains with hydration, and from the re-orientation of the β-sheet crystals and network chains with contraction. In *Nephila* silk, the network chains retain their ordered structure, and the modest fall in birefringence is due to the partial reorientation of stable secondary structures. In *Araneus* silk, the dramatic drop in birefringence reflects the melting of extended,

Table 3. Birefringence reading for dry, wetted/restrained, and supercontracted MA silk from *Araneus diadematus* and *Nephila clavipes*

	A. diadematus	*N. clavipes*
Dry birefringence	0.0247±0.017 (*N*=12)	0.0385±0.017 (*N*=12)
Wetted, restrained birefringence	0.0210±0.0006 (*N*=10)	0.038±0.0014 (*N*=12)
Supercontracted	0.00610±0.00001 (*N*=6)	0.018±0.00001 (*N*=9)

The errors represent ± 1 standard deviation. Differences are statistically significant at $P<0.05$.

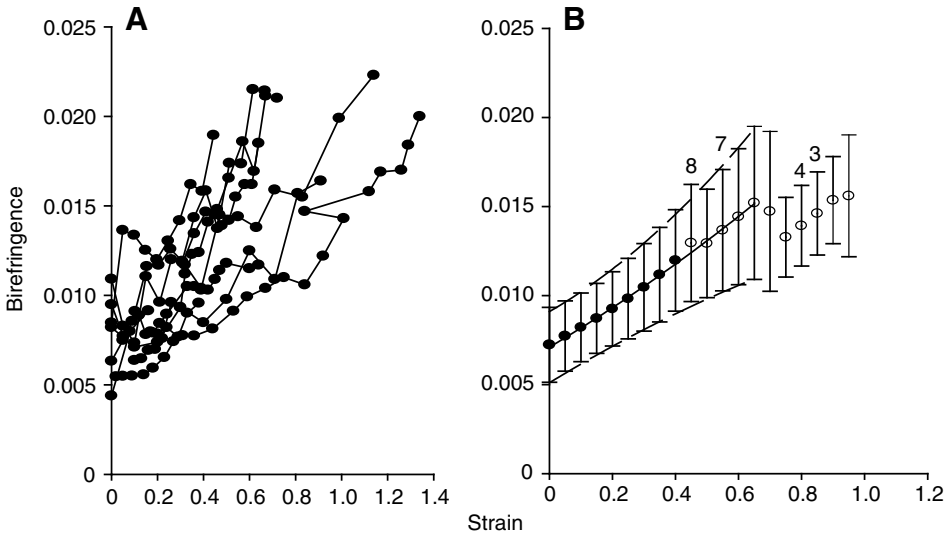

Fig. 8. Birefringence measurements *versus* strain for supercontracted MA silk from *Araneus*. (A) The complete data set and (B) the average behaviour of the data set. Predicted values were averaged from all the curves for which a value was available. Filled circles represent values averaged from all nine tests and open circles represent values averaged from all tests for which a value at that extension was available. The numbers above each data point represent the number of curves included in the average. The calculated curve is fitted to the second order polynomial, $y=0.0122x+0.0070$, $r^2=0.99$. Error bars are one standard deviation. Each sample was from a different spider.

amorphous network chains, which allows a reorientation of the β-sheet crystals and also allows the network chains to relax to an essentially isotropic state. These dramatic changes in network structure with supercontraction must have important consequences, and the mechanical tests clearly reveal dramatic differences in material properties.

Fig. 6 clearly shows that there is essentially no overlap in values between the two populations of hydrated silk fibres. Thus, in spite of the enormous variability of the silk samples (Figs 4 and 5), the difference in the hydration-induced changes of hydrogen bonding within the network chains is so large that the two silks become entirely different in their mechanical properties. The initial modulus of *Nephila* MA silk dropped by a factor of 113 when supercontracted, but that of *Araneus* MA silk fell by a factor of 1010. This eightfold difference in stiffness change between *Nephila* and *Araneus* implies stiffer, more ordered network chains in *Nephila* MA silk, and any of the proposed secondary structures could account for this difference. Proline is a known β-sheet breaker and could act to disrupt the formation of crystalline structure in the network, and *Araneus* MA silk, with its high proline content, should thus have a more amorphous network. On contact with water, the *Araneus* MA silk would swell to a greater degree, and the modulus would be lower once supercontracted because the network chains become kinetically free.

Fig. 7A clearly shows how stiffness varies with strain for both silks. *Nephila* MA silk retains a higher fraction of its dry stiffness, whereas the stiffness of *Araneus* MA silk increases much more with strain. The log stiffness *versus* strain plot shown in Fig. 7B more clearly documents these changes in stiffness. Initially, hydrated *Nephila* silk is 10 times stiffer than hydrated *Araneus* MA silk. At a strain of 0.65, the stiffness of the *Araneus* silk has increased, and the difference in stiffness between *Nephila* and *Araneus* is reduced to 1.66. The fact that *Nephila* MA silk retains more of its initial dry stiffness indicates the presence of a more ordered fibroin network, and provides evidence for the existence of ordered structure in the glycine-rich network chains. The rise in stiffness in *Nephila* silk is probably due primarily to the reorientation of both the poly-alanine crystals and the ordered structures within the network chains.

Araneus MA silk exhibits a much more pronounced drop in stiffness upon hydration, and the low stiffness seen at lower strains likely reflects the fact that the network chains are kinetically free. As the network chains are oriented with strain, the stiffness of the

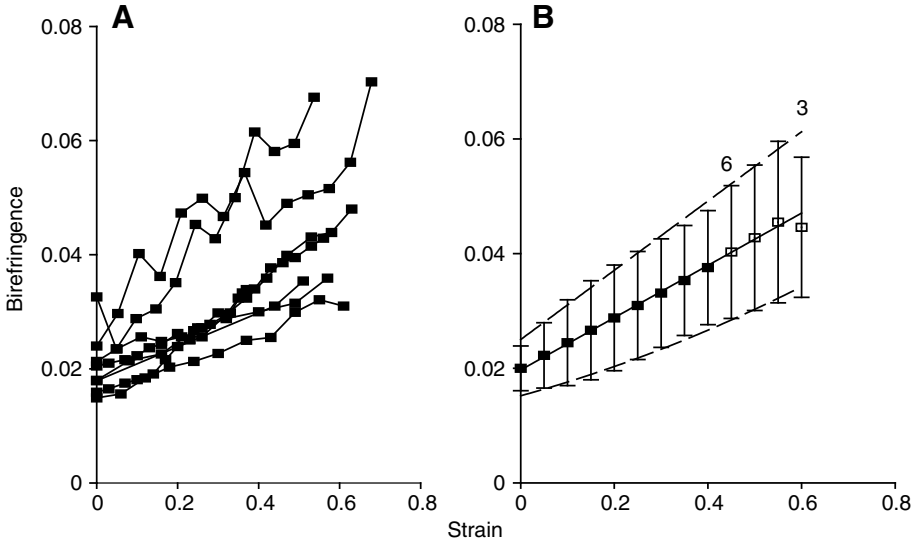

Fig. 9. Birefringence measurements *versus* strain for supercontracted MA silk from *Nephila* (A)The complete data set and (B) the average behaviour of the data set. Predicted values were averaged from all the curves for which a value was available. Filled squares represent values averaged from all seven tests and open squares represent values averaged from all tests for which a value at that extension was available. The numbers above each data point represent the number of curves included in the average. The calculated average behaviour is fitted to the linear regression, $y=0.0456x^2+0.0197$, $r^2=1$. Error bars are one standard deviation. Each sample was from a different spider.

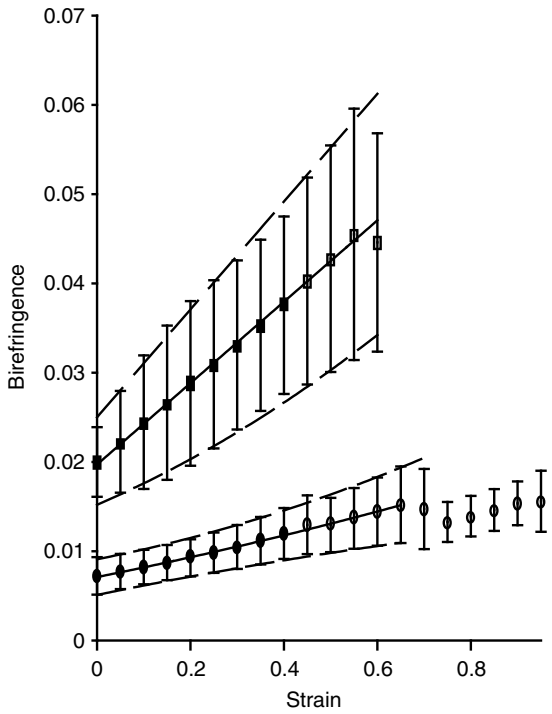

Fig. 10. The average birefringence curves in Fig. 7B (*Araneus*) and Fig. 4B (*Nephila*) are presented on the same axis for direct comparison.

Araneus fibre rapidly approaches that of the *Nephila* silk, probably because of the non-Gaussian behaviour of the glycine-proline-rich network chains. It is, therefore, expected that at a strain of this level the *Araneus* silk may still be dominated by entropic elasticity.

The differences in network structure indicated by the mechanical properties of the supercontracted silks are also reflected by the change of birefringence with strain (Figs 8–10). Supercontracted *Nephila* MA silk retains more molecular order than does *Araneus*, and therefore it was hypothesized that the birefringence of the *Nephila* silk would be both higher and exhibit a higher increase with strain than the *Araneus* silk. Indeed, this was found to be the case; the initial hydrated birefringence of *Nephila* MA silk was three times higher than that of *Araneus* (Table 3). In addition, while there was a high degree of variability in the birefringence-strain data, Fig. 10 clearly shows that there was no overlap between the two data sets. The rapid rise in birefringence with extension seen in *Nephila* MA silk may be due to existing structures in ordered network chains re-orientating with strain. In the case of *Araneus*, the smaller rise in birefringence is likely due to the amorphous network chains unwinding with strain. In fact, similar birefringence-strain data has previously been published in a study that attempted to attribute changes in birefringence to aspects of a two-phase model for a silk network (Gosline et al., 1995). In that study, the predicted birefringence for a random polymer network in which network chains occupy 88% of the network volume was calculated, and subtracted from the measured values of birefringence. The result suggests that the poly-alanine crystals re-orientate with the first 30% of strain, after which they are essentially fully oriented to the fibre axis.

There are two basic models for the structure of the glycine-rich network chains: (1) the network chains are kinetically-free, random-coils, and they sample many possible conformations over a small time scale; (2) the network chains form stable secondary structures, which have been proposed to be non-periodic lattice crystals, 3_1 helices, or β-sheets. The first model is based on the fact that supercontracted *Araneus* MA silks are entropic (Gosline et al., 1984), and their properties can be predicted from the theory of rubber elasticity. The second model is based on NMR and X-ray data that have been used to propose non-periodic lattice crystals and/or 3_1 helices as possible stable secondary structures. In this study we have shown that in the dry state, the properties of both *Araneus* and *Nephila* MA silks are dominated by the stabilizing effect of inter and intra-chain hydrogen bonds, both within the poly-alanine β-sheets and within the glycine-rich network chains. These hydrogen bonded structures are responsible for the high initial stiffness (10 GPa) of both silks. However, once hydrated, MA silks swell, shrinking in length and increasing in volume in a process termed supercontraction. This phenomenon is associated with a dramatic drop in the initial modulus for both silks, but the results discussed above provide strong evidence that there are dramatic differences in the nature and extent of the structural organization of the glycine-rich network chains of these two silks. These differences are almost certainly associated with differences in the strength of the hydrogen bonds that form in the proline-deficient and proline-rich network chains.

In Fig. 2C we presented a hypothetical distribution of hydrogen-bond energy, or bond strength that we created to illustrate our hypotheses for the state of the proline-rich (+Pro) or proline-deficient (–Pro) silk networks, both in the dry and in the hydrated states. The key feature of our model was that the peak representing the distribution of hydrogen bond energies of proline-rich network chains is shifted left to lower energies and is much broader than the distribution of hydrogen bond energies of proline-deficient network chains. These bond energy distributions represent our hypothesis that the proline-rich network chains are essentially random-coils, and that the proline-deficient sequences form stable secondary structures. The figure shows distributions for these hydrogen-bonds for silk fibres in water, and the key features were that the energy distribution for the proline-rich network chains shift to much lower energies, such that thermal energy, kT, is sufficient to induce extensive mobility, whereas the distribution for proline-deficient network chains shift to lower energies but not low enough to induce wide-spread mobility. The mechanical and optical data presented in this study are entirely consistent with this hypothetical energy distribution, and it likely, therefore, forms a useful starting basis for understanding the structure and dynamics of the protein networks in these two types of MA silk. However, in spite of the fact that there is a good fit of our data to this bond energy scheme, it is clear that the relationship is entirely qualitative and much remains to be learned about the structure and dynamics of spider silk networks. In particular, the mechanical and optical properties of intact fibres presented in this paper measure the average properties, but do not take into account any hierarchal sub-structures within silk fibres.

Indeed, using a combination of light microscopy and scanning electron microscopy, Vollrath et al. (Vollrath et al., 1996) observed that *Nephila clavipes* MA silk has a distinct skin–core structure when supercontracted in urea. van Beek et al. (van Beek et al., 2002) further refined the idea of a skin–core structure based on NMR data of *Nephila edulis* MA silk. They proposed that this silk is composed of axially aligned fibrillar substructures covered by a hard skin; each fibril is composed of a matrix of 3_1-helices crosslinked by poly-alanine β-sheet crystals. Sponner et al. (Sponner et al., 2005) stained cross-sections of *Nephila clavipes* MA silk fibres with antibodies to both spidroin-1 and spidroin-2, and immuno-electron microscopy

confirmed the presence of a skin–core structure. The presence of a mixture of spidroin-1 and 2 seems to promote a hierarchical structure in MA silk on a larger scale than the nano-scale composite of β-sheet crystals and network chains seen by X-ray or NMR studies. This skin–core structure is composed of a thin skin, roughly 0.5 μm thick of spidroin-1, and a core region containing both spidroin-1 and 2. The spinning process apparently induces a polymer phase separation that aggregates spidroin-2 and promotes the formation of fibrils (~200 nm diameter) within the core. To date, similar structural studies using X-ray crystallography, NMR and immuno-staining have not been done on *Araneus* MA silk, in which only spidroin-2 fibroins are expressed. It remains to be seen if such studies on proline-rich silks will yield additional insights into the relationship between the molecular structure of the polymer network, hierarchical skin–core structures, and the material properties of MA silks.

Conclusions

Araneus MA silk contains essentially amorphous network chains, which become highly mobile when hydrated. It exhibits rubber-like elasticity (Gosline et al., 1984), and random-network models based on rubber elasticity appear to accurately portray the behaviour of this silk. Thus, the decrease in conformational entropy that occurs by stretching a hydrated *Araneus* MA silk fibre provides the energy necessary to drive the elastic recoil when the stretching force is removed. Conversely, random-network models do not appear to provide an appropriate model for the network chains in *Nephila* MA silk. Comparison of the mechanical and optical properties of hydrated *Nephila* and *Araneus* MA silk clearly indicate that the network chains in *Nephila* silk are quite stiff and ordered in both the dry and hydrated states. Thus with the presence of stable secondary structures in the hydrated *Nephila* MA silk network, the elastic mechanism in this silk is likely to be dominated by changes in bond energy associated with the deformation of rigid or semi-rigid structures. Thus, our results indicate that these two silks have fundamentally different network structures, and if this is correct, then a study to examine the thermodynamics of their elasticity should clearly reveal these differences. Thermoelastic experiments to determine the nature of their elastic mechanism are presented in another paper (Savage and Gosline, 2008).

This study was supported by Discovery Grant (6934-04 from the Canadian Natural Sciences and Engineering Research Council to J.M.G.

REFERENCES

Andersen, S. O. (1970). Amino acid composition of spider silks. *Comp. Biochem. Physiol.* **35**, 705-711.
Becker, M. A., Mahoney, D. V., Lenhert, P. G., Eby, R. K., Kaplan, D. and Adams, W. W. (1994). X-ray moduli of silk fibers from *Nephila clavipes* and *Bombyx mori*. *Silk Polymers* **544**, 185-195.
Cunnliff, P. M., Fossey, S. A., Auerbach, A., Song, J. W., Kaplan, D. L., Adams, W., Eby, D. and Vezie, D. (1994). Mechanical and thermal properties of dragline silk from *Nephila clavipes*. *Polymers Adv. Technol.* **5**, 401-410.
Denny, M. W. (1976). The physical properties of spider's silk and their role in the design of orb-webs. *J. Exp. Biol.* **65**, 483-506.
Edwards, H. G. M. and Farwell, D. W. (1995). Raman-spectroscopic studies of silk. *J. Raman Spectrosc.* **26**, 901-909.
Eles, P. T. and Michal, C. A. (2004a). A DECODER NMR study of backbone orientation in *Nephila* clavipes dragline silk under varying strain and draw rate. *Biomacromolecules* **5**, 661-665.
Eles, P. T. and Michal, C. A. (2004b). Strain dependent local phase transitions observed during controlled supercontraction reveal mechanisms in spider silk. *Macromolecules* **37**, 1342-1345.
Fornes, R. E., Work, R. W. and Morosoff, N. (1983). Molecular orientation of spider silks in the natural and supercontracted states. *J. Polymer Sci.* **21**, 1163-1172.
Fraser, R. D. B. and MacRae, T. P. (1973). *Conformation in Fibrous Proteins an Relate Synthetic Polypeptides*. New York: Academic Press.
Fudge, D., Gardner, K. H., Forsyth, V. T., Riekel, C. and Gosline, J. (2003). The mechanical properties of hydrated intermediate filaments: insights from hagfish slime threads. *Biophys. J.* **85**, 2015-2027.
Gatesy, J., Hayashi, C., Motriuk, D., Woods, J. and Lewis, R. (2001). Extreme diversity, conservation, and convergence of spider silk fibroin sequences. *Science* **291**, 2603-2605.
Gosline, J. M., Denny, M. W. and Edwin, D. M. (1984). Spider silk as rubber. *Nature* **309**, 551-552.
Gosline, J. M., Pollak, C. C., Guerette, P. A., Cheng, A., DeMont, M. E. and Denny, M. W. (1994). Elastomeric network models for the frame and viscid silks from the orb web of the spider *Araneus diadematus*. In *ACS Symposium Series*. Vol. 544 (ed. D. L. Kaplan, W. W. Adams, B. Farmer and C. Viney), pp. 329-341. Charlottesville, VA: American Chemical Society.
Gosline, J., Nichols, C., Guerette, P., Cheng, A. and Katz, S. (1995). The macromolecular design of spiders' silks. In *Biomimetics: Design and Processing of Materials* (ed. M. Sarikaya and I. A. Aksay), pp. 237-261. Woodbury, NY: American Institute of Physics.
Gosline, J. M., Guerette, P. A., Ortlepp, C. S. and Savage, K. N. (1999). The mechanical design of spider silks: from fibroin sequence to mechanical function. *J. Exp. Biol.* **202**, 3295-3303.
Grubb, D. T. and Jelinski, L. W. (1997). Fiber morphology of spider silk: the effects of tensile deformation. *Macromolecules* **30**, 2860-2867.
Guerette, P. A., Ginzinger, D. G., Weber, B. H. and Gosline, J. M. (1996). Silk properties determined by gland-specific expression of a spider fibroin gene family. *Science* **272**, 112-115.
Hayashi, C. Y. and Lewis, R. V. (1998). Evidence from flagelliform silk cDNA for the structural basis of elasticity and modular nature of spider silks. *J. Mol. Biol.* **275**, 773-784.
Kummerlen, J., van Beek, J. D., Vollrath, F. and Meier, B. H. (1996). Local structure in spider dragline silk investigated by two-dimensional spin-diffusion nuclear magnetic resonance. *Macromolecules* **29**, 2920-2928.
Ortlepp, C. S. and Gosline, J. M. (2004). Consequences of forced silking. *Biomacromolecules* **5**, 727-731.
Perez-Rigueiro, J., Elices, M., Plaza, G., Real, I. and Guinea, G. V. (2005). The effect of spinning forces on spider silk properties. *J. Exp. Biol.* **208**, 2633-2639.
Rauscher, S., Baud, S., Miao, M., Keeley, F. W. and Pomes, R. (2006). Proline and glycine control protein self-organization into elastomeric or amyloid fibrils. *Structure* **14**, 1667-1676.
Riekel, C., Branden, C., Craig, C., Ferrero, C., Heidelbach, F. and Muller, M. (1999). Aspects of X-ray diffraction on single spider fibers. *Int. J. Biol. Macromol.* **24**, 179-186.
Savage, K. N. and Gosline, J. M. (2008). The role of proline in the elastic mechanism of hydrated spider silks. *J. Exp. Biol.* **211**, 1948-1957.
Savage, K. N., Guerette, P. A. and Gosline, J. M. (2004). Supercontraction stress in spider webs. *Biomacromolecules* **5**, 675-679.
Shao, Z. Z., Young, R. J. and Vollrath, F. (1999). The effect of solvents on spider silk studied by mechanical testing and single-fibre Raman spectroscopy. *Intern. J. Biol. Macromol.* **24**, 295-300.
Sheu, H. S., Phyu, K. W., Jean, Y. C., Chiang, Y. P., Tso, I. M., Wu, H. C., Yang, J. C. and Ferng, S. L. (2004). Lattice deformation and thermal stability of crystals in spider silk. *Int. J. Biol. Macromol.* **34**, 325-331.
Simmons, A. H., Michal, C. A. and Jelinski, L. W. (1996). Molecular orientation and two-component nature of the crystalline fraction of spider dragline silk, *Science* **271**, 84-87.
Sponner, A., Unger, E., Grosse, F. and Klaus, W. (2005). Differential polymerization of the two main protein components of dragline silk during fibre spinning. *Nat. Mat.* **4**, 772-775.
Stauffer, S. L., Coguill, S. L. and Lewis, R. (1994). Comparison of physical properties of three silks from *Nephila clavipes* and *Araneus gemmoides*. *J. Arachnol.* **22**, 5-11.
Termonia, Y. (1994). Molecular modeling of spider silk elasticity. *Macromolecules* **27**, 7378-7381.
Thiel, B. L., Guess, K. B. and Viney, C. (1997). Non-periodic lattice crystals in the hierarchical microstructure of spider (major ampullate) silk. *Biopolymers* **41**, 703-719.
van Beek, J. D., Hess, S., Vollrath, F. and Meier, B. H. (2002). The molecular structure of spider dragline silk: folding and orientation of the protein backbone. *Proc. Natl. Acad. Sci. USA* **99**, 10266-10271.
Vollrath, F., Holtet, T., Thogerson, H. C. and Frishe, S. (1996). Structural organization of spider silk. *Proc. R. Soc. Lond. B Biol. Sci.* **263**, 147-151.
Warwicker, J. O. (1960). Comparative studies of fibroins II. The crystal structures of various fibroins. *J. Mol. Biol.* **2**, 350-362.
Witt, P. N. (1971). Instructions for working with web-building spiders in the laboratory. *BioScience* **21**, 23-25.
Work, R. W. (1977). Dimensions, birefringences, and force-elongation behavior of major and minor ampullate silk fibers from orb-web-spinning spiders: the effects of wetting on these properties. *Text. Res. J.* **47**, 650-662.
Work, R. W. (1981). A comparative study of the supercontraction of major ampullate silk fibers of orb-web-building spiders (Araneae). *J. Arachnol.* **9**, 299-308.
Work, R. W. (1982). A physio-chemical study of the supercontraction of spider major ampullate silk fibers. *Text. Res. J.* **52**, 349-356.
Work, R. W. (1985). Viscoelastic behaviour and wet supercontraction of major ampullate silk fibres of certain orb-web-building spiders (Araneae). *J. Exp. Biol.* **118**, 379-404.
Work, R. W. and Young, C. T. (1987). The amino-acid compositions of major and minor ampullate silks of certain orb-web-building spiders (Araneae, Araneidae). *J. Arachnol.* **15**, 65-80.
Yang, Z., Grubb, D. T. and Jelinski, L. W. (1997). Small-angle X-ray scattering of spider dragline silk. *Macromolecules* **30**, 8254-8261.